Energy Science & Engineering

Open Access

REVIEW

Advances in understanding the surface chemistry of lignocellulosic biomass via time-of-flight secondary ion mass spectrometry

Allison Tolbert[1,2] and Arthur J. Ragauskas[2,3,4]

[1]School of Chemistry and Biochemistry & Renewable Bioproducts Institute , Georgia Institute of Technology, Atlanta, GA, USA 30332
[2]BioEnergy Science Center (BESC), Biosciences Division , Oak Ridge National Laboratory, Oak Ridge, TN, USA 37830
[3]Joint Institute of Biological Sciences, Biosciences Division , Oak Ridge National Laboratory, Oak Ridge, TN, USA 37831
[4]Department of Chemical and Biomolecular Engineering, Department of Forestry, Wildlife, and Fisheries, & Center for Renewable Carbon, University of Tennessee, Knoxville, TN, USA 37996

Keywords
Enzymatic hydrolysis, genetic modification, lignocellulosic biomass, pretreatment, secondary ions, time-of-flight secondary ion mass spectrometry

Correspondence
Arthur Ragauskas, Oak Ridge National Laboratory, PO Box 2008 MS6341, Oak Ridge, TN 37831-6341. E-mail: aragausk@utk.edu

Funding Information
Allison K. Tolbert is grateful for the financial support from the Paper Science & Engineering (PSE) fellowship program at the Renewable Bioproducts Institute at Georgia Institute of Technology.

Received: 4 August 2016; Revised: 28 September 2016; Accepted: 21 October 2016

doi: 10.1002/ese3.144

Abstract

Overcoming the natural recalcitrance of lignocellulosic biomass is necessary in order to efficiently convert biomass into biofuels or biomaterials and many times this requires some type of chemical pretreatment and/or biological treatment. While bulk chemical analysis is the traditional method of determining the impact a treatment has on biomass, the chemistry on the surface of the sample can differ from the bulk chemistry. Specifically, enzymes and microorganisms bind to the surface of the biomass and their efficiency could be greatly impacted by the chemistry of the surface. Therefore, it is important to study and understand the chemistry of the biomass at the surface. Time-of-flight secondary ion mass spectrometry (ToF-SIMS) is a powerful tool that can spectrally and spatially analyze the surface chemistry of a sample. This review discusses the advances in understanding lignocellulosic biomass surface chemistry using the ToF-SIMS by addressing the instrument parameters, biomass sample preparation, and characteristic lignocellulosic ion fragmentation peaks along with their typical location in the plant cell wall. The use of the ToF-SIMS in detecting chemical changes due to chemical pretreatments, microbial treatments, and physical or genetic modifications is discussed along with possible future applications of the instrument in lignocellulosic biomass studies.

Introduction

Lignocellulosic biomass is a valuable renewable resource that is primarily composed of cellulose, hemicellulose, and lignin. The key hindrance to the utilization and conversion of these biopolymers into biofuels and bioproducts via the biological conversion platform is the natural recalcitrance of the biomass. Through chemical, physical, and/or biological pretreatments along with genetic modifications, progress has been made toward reducing biomass recalcitrance and accessing lignocellulosic polymers. These various processes modify the structure and/or chemistry of the plant cell walls by altering one or more of the polymers of the plant cell wall and increasing the accessibility to cellulose. Currently, the fundamental principles of biomass recalcitrance are under active investigation so as to facilitate practical conversion of plant polysaccharides into simple sugars that can readily be fermented to ethanol and related alcohols. It is generally acknowledged that comprehensive analytical biomass analysis is key to understanding the principles of recalcitrance. High-performance liquid chromatography (HPLC), gel permeation chromatography (GPC), nuclear magnetic resonance (NMR), Fourier transform infrared (FT-IR) spectroscopy, X-ray photoelectron spectroscopy (XPS), scanning transmission X-ray microscopy (STXM), and ultraviolet (UV) spectrophotometry are typical analysis instruments for characterizing biomass and its molecular

components, for example, the degree of polymerization, molecular weight distribution, cellulose crystallinity, accessibility, lignin structural characteristics, and cellulose accessibility to cellulase [1–5]. Electron microscopy tools, like transmission electron microscopy (TEM), scanning electron microscopy (SEM), and atomic force microscopy (AFM), have also been developed to analyze the morphological changes to biomass samples [6–9].

Time-of-flight secondary ion mass spectrometry (ToF-SIMS) is a mass spectrometry tool that is matrix free with regards to ionization of a sample's surface and detects lower molecular weight fragmented species in high mass resolution spectra and spatial mapping [10, 11]. Some advantages to using a ToF-SIMS are direct analysis of solid samples [12], minimal sample preparation steps [13], and low surface damage in the range of a few nanometers [14]. Also, the mass spectral imaging is extremely useful in mapping selected secondary ions on a heterogeneous surface, like lignocellulosic biomass [11]. The relative amounts of cellulose and lignin and their location in the cell walls on the surface of a biomass samples are important in understanding how the plant cell wall structure is impacted due to various treatments or modifications. In addition, the deconstruction of cellulose by cellulase is a surface-dominated process and, hence, there is a compelling need to understand the chemical structure of the surface of biomass. There have been a number of advances to the use of the ToF-SIMS since Belu et al. [15] published a comprehensive review of ToF-SIMS covered basic principles and applications for the instrument. This is especially true in relation to characterizing lignocellulosic biomass via ToF-SIMS. This study covers the principles of the instrument used to study biomass along with sample preparation, key lignocellulosic secondary ions and their location in the cell wall, and detecting various biomass modifications using this methodology.

Instrument Principles

Time-of-flight secondary ion mass spectrometry functions by emitting a pulsed primary ion beam from a liquid metal ion gun, which is rastered across the surface of the sample ejecting positive, negative, and neutral secondary ions (Fig. 1). There are different liquid metals for the pulsed primary ion beam, including gallium [11, 14, 16–18], gold [19, 20], and bismuth [10, 21–26]. Clustered ion sources, like Bi_3^{2+}, are capable of increasing the yield of higher molecular weight secondary ions while not damaging the sample surface more [15]. It is important to be aware of the instruments' primary ion source as it can significantly impact the intensities of the secondary ion peaks in the resulting spectra [15]. The primary ion beam utilizes energy between 1 and 25 keV, which allows enough

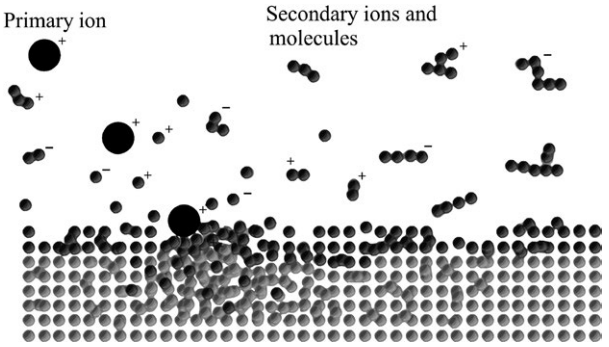

Figure 1. A schematic drawing of the formation of secondary ions from the sample surface after primary ion impact. Reprinted from Belu et al. [15] with permission from Elsevier.

force to bombard the sample surface and eject the secondary ions from the top 1–2 nm of the sample [14, 15, 25].

The ToF-SIMS spectra are formed after the secondary ions are detected by the ToF-SIMS analyzer and separated according to their mass-to-charge (m/z) ratio. The specific secondary ion peaks are selected in the calibrated spectra and can result in relative ion counts/intensities, or spatial mapping of ions, depending on the mode setting (bunched mode for high-resolution spectra and burst/burst alignment mode for images, Fig. 2) [27]. Some of the ToF-SIMS settings depend on the type of sample being analyzed. For example, with biomass the ToF-SIMS analyzer is set to detect positive ions as all developed libraries for lignocellulosic biomass are for cations. Also, the bombardment of primary ions on a biomass sample easily results in surface charging, which is reduced by using a low-energy pulsed electron gun, or a floodgun [14].

While the settings might need to be sample specific, the interpretation of the ToF-SIMS data is likewise dependent on the sample. Spectra of different locations on a sample are slightly different in the total number of secondary ions detected, and as a reference, some studies report a mass resolution (M/ΔM) range. The mass resolution is dependent on the surface roughness, and varied roughness on a sample could result in different total ion counts. When analyzing biomass, the M/ΔM for m/z 23 or 91 has been reported[10, 13]; for example, at m/z 91, Goacher et al. [13] reported mass resolutions of ~3000–5000 and ~250–300 for bunched mode and burst alignment mode, respectively. Prior to selecting specific peaks, ToF-SIMS spectra need to be calibrated. For lignocellulosic biomass analysis, a few typical ions used for calibration are CH_3^+, H_3O^+, $C_2H_3^+$, $C_3H_5^+$, and $C_5H_7^+$ [10, 13, 21–23, 26].

After the spectra are calibrated and the specific characteristic ion peaks selected, the ion intensities for these

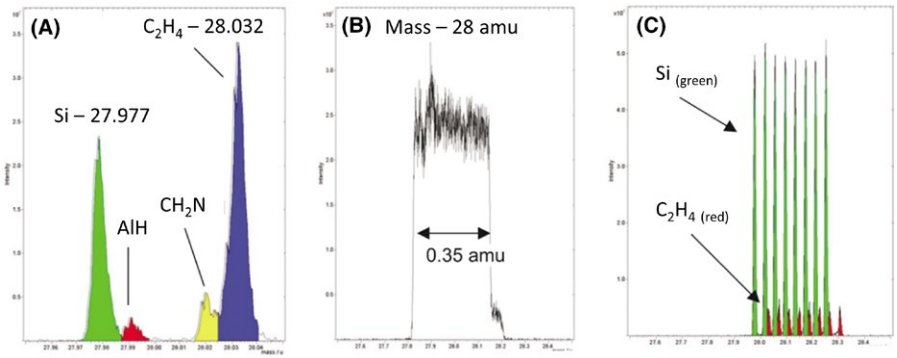

Figure 2. Mass spectra examples for the (A) bunched spectral and (B–C) burst/burst alignment imaging operational modes. Reproduced in part from Sodhi [27] with permission of The Royal Society of Chemistry.

peaks are typically normalized to the total ion intensity detected by the analyzer. The normalized ion intensities can be used for further direct comparison analysis, ratios, and/or multivariate analysis, like principal component analysis (PCA) which was used by Goacher et al. [13] to develop a lignocellulosic biomass library. The spectra for spatial images likewise need to be calibrated prior to the characteristic ion peaks selection. ToF-SIMS 2D imaging can potentially spatially resolve the cell wall chemically to under 1 μm and occur up to distances of approximately 300–400 nm [10, 24]. ToF-SIMS detects the location of emitted secondary ions and creates pixels based on this information to form spatial mapping of the total ions or specifically selected ions. For biomass, an image based on chemical ions helps determine location of high- or low-intensity lignocellulose ions on the cell wall.

There have been several recent advances to the ToF-SIMS technique for analyzing biomass. Jung et al. stacked a series of 2D ToF-SIMS images to form a 3D molecular image (Fig. 3) by removing the previous analyzed top layer of the sample with a sputtering beam, like O_2^+ and C_{60}^+ [24, 25]. This method has the potential to be extremely valuable in gaining insight into the interaction between a biomass sample and enzymes or microbes, especially in detecting the vertical distance the enzyme/microbe penetrates [24]. It is also possible to conduct 3D analysis by cutting subsequent layers off of the biomass if the previous analysis position can be easily identified, but the layers would be tens of micrometers apart from each other [19]. Another advancement utilizes the development of a cryo-ToF-SIMS/SEM system that is capable of analyzing frozen-hydrated biomass samples to minimize the movement of water soluble chemicals during the drying process [19]. This new system works by moving a holder that the biomass is mounted on between a glove box and a cryo-SEM or a cryo-ToF-SIMS [19].

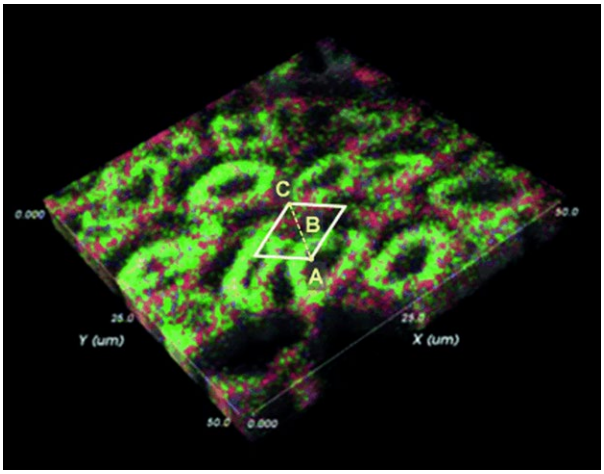

Figure 3. Time-of-flight secondary ion mass spectrometry 3D image of poplar tension wood stem cross-section, where cellulose (green pixels) and lignin (red pixels) are spatially distributed. The square edges are 50 μm long and the image is composed of 30 2D images stacked. Reprinted (adapted) with permission from Jung et al. [24]. Copyright (2012) John Wiley & Sons, Inc.

Biomass Sample Preparation

All analytical instruments require samples to be prepared in specific ways in order to accurately analyzed them. The following are general preparation descriptions necessary for lignocellulosic biomass prior to ToF-SIMS analysis, specific details can be found in the subsections below. First, biomass samples need to fit correctly into the ToF-SIMS mounting stage either through milling or sectioning the sample to a smaller size. Second, the removal of extractives, nonstructural biomass material, is necessary for most ToF-SIMS analyzes and it can be accomplished using a number of different procedures. Additional rinsing or washing might be required to

remove any chemical residue after a pretreatment and/or enzymatic hydrolysis. Once the samples are dried, they are then ready for analysis via the ToF-SIMS. Below are various processes for milling and sectioning the biomass along with different biomass extractions, ways to rinse postenzymatic hydrolysis, and drying techniques used in various studies.

Milling and sectioning

Time-of-flight secondary ion mass spectrometry can analyze biomass samples that are prepared in various ways, including milled wood or powder, sectioned tissue, and small blocks of wood [11, 16, 17, 28]. The size of milled biomass for ToF-SIMS studies has varied from 0.149 to 0.841 mm [16, 18, 21, 22]. A benefit to using milled wood is that it helps reduce the heterogeneous nature of the wood found within the different cell wall regions and different zones, like heartwood and sapwood [22]. Milled biomass can be compressed into wood powder pellets or attached to adhesive tape prior to ToF-SIMS analysis [12, 22, 26]. If the adhesive tape is used, it is important to know the ToF-SIMS spectra of the tape in order to identify any peaks that overlap with those characteristic of lignocellulose [12]. Saito et al. [11, 14] originally pressed the powdered milled wood lignin onto indium foil sheet, but to attain even a higher mass resolution, the sample mixed with acetone was dropped onto a silicone wafer where it dried; the drop-dried method resulted in a flatter, homogeneous milled biomass sample for ToF-SIMS analysis.

The sectioning of plant tissue from whole stems or small blocks of wood typically occurs on a cryotome or a microtome. It is important to be aware of the materials used to section the biomass so minimal damage occurs during the cutting process. A previous study showed that a cryomicrotome using a steel knife collapses the plant cell walls, while a double-edged razor blade results in varied section thickness [29]. Tokareva et al. [29] went on to determine that a disposable microtome blade can be used for biomass sectioning, but it must first be cleaned to remove any polytetrafluoroethylene (PTFE) on the blade that might contaminate the samples. A cleaned diamond knife on a microtome is also a useful tool to cut biomass sections [13]. There are various methods used to clean blades and knives that typically involve solvents, including acetone [10, 13], dichloromethane, and ethanol [16], and dichloromethane in a high-intensity ultrasonic processor [29]. The cross- and transversal sections can be cut to various micrometer thickness like 12 μm [25], 20 μm [30], and 50 μm [10, 16]. Note that different cutting techniques might result in microtome-induced smearing and debris leading to a loss in spatial resolution; to correct for this, the first few layers of the sample can be removed with a sputtering ion beam [25].

Biomass studies incorporating a pretreatment followed by enzymatic hydrolysis typically utilizes milled biomass, sawdust, or woodchips. A study analyzing 0.841-mm ground poplar and 50-μm-thick poplar cross-sections via FT-IR and carbohydrate analysis determined that the ground and section poplar were comparable chemically [16]. This indicates that it is inconsequential whether the sample biomass is milled or sectioned, and the actual limiting factor for biomass size preparation is for it to fit in the ToF-SIMS mounting stage. While ToF-SIMS can analyze both milled and sectioned samples, the cell walls of sectioned biomass have greater probability of being intact for ToF-SIMS imaging than the milled biomass. Otherwise, the milling or cutting process is dependent on the research study and the biomass; for example, switchgrass would have to fully be encased in embedding material to obtain cross-sections via a microtome, but a cryotome would easily section juvenile poplar that is mounted to a metal stage. Prior to analysis, the samples most often have the extractives removed for simplified ToF-SIMS analysis.

Removing the extractives

Extractives are essentially chemicals that do not contribute to the structure of the cell walls in the biomass [31]. They typically fall into two categories, water soluble and ethanol soluble materials [31]. These materials can include inorganics, waxes, nitrogen-based compounds, and nonstructural sugars [31]. Fardim and Durán proposed ToF-SIMS peak assignments for seven free fatty acids, eight fatty acid salts, and three sterols all over *m/z* 200 [32], whereas Goacher et al. [12] developed a list of 32 low mass peaks (under *m/z* 200) that "distinguished unextracted from extracted lignocelluloses samples."

The main reason for the removal of biomass extractives is due to their ability to mask the detection of secondary ions from lignin and cellulose [29]. Goacher et al. [12] compared unextracted and extracted spruce, aspen, and *Arabidopsis* and determined that an observed change in the amount of lignin ions could actually be caused by a change in extractive content on the unextracted biomass sample. Phenolic extractives, in particular, may be interfering with the instrument's ability to accurately detect lignin [28]. For this reason, the analysis of unextracted biomass may result in mass interferences or alter peak proportions which could negatively impact peak assignments [13].

This stresses the importance of extraction, especially when trying to identify lignin fragmentation ions of a sample's surface. Various biomass extraction techniques,

which typically are performed for 4–12 h or even longer depending on the procedure, include solvent solutions using acetone, dichloromethane, ethanol, and toluene in different concentrations, some of which are detailed in Table 1. Samples need to be dried prior to analysis, but further rinsing might be required to remove any traces of buffers if the samples underwent enzymatic hydrolysis.

Rinsing after enzymatic hydrolysis

In enzymatic reactions, buffers maintain the pH, but they produce inorganic peaks that interfere with lignocellulosic peaks [33]. Salts can negatively impact the ToF-SIMS spectra as samples not exposed to buffers result in relatively low sodium ion peaks [12]. Buffers typically have been removed by rinsing with distilled water; Braham and Goacher determined that rinsing wood with acetic acid removes more buffer-related salt ions, specifically potassium and sodium, than distilled water [33]. Nevertheless, distilled water is still an effective way to reduce the buffer salts on the samples surface [33]. Using potassium salts instead of sodium salts to prepare pH buffers is better as both acetic acid and distilled water are more efficient in removing potassium salts and K-buffer produces fewer interferences with the characteristic lignocellulosic peaks [33]. After rinsing, biomass samples then undergo a drying process like other pretreated or extractive-free samples.

Drying the sample

Biomass samples for ToF-SIMS analysis need to be dried prior to loading into the instrument. Different studies have dried the biomass through freeze drying [17, 30], critical point drying [34], and air drying [12, 16, 22, 23], in addition to oven drying at 60°C [22]. Tokareva et al. [29] studied Norway spruce that was freeze-dried, air-dried, acetone extracted with nitrogen flow drying, and ethanol-acetone dehydration with critical point drying to determine what drying process gave better results (Table 2). The analysis of the freeze-dried and air-dried samples revealed extractives on the sample surface that were masking the ion signals from the major lignocellulosic components [29]. Therefore, the samples that were dried via critical point drying or nitrogen flow after extraction were accurately prepared for ToF-SIMS analysis and it was determined that either drying technique would be appropriate to use [29]. Other studies tend to differ the biomass drying process from those listed in Table 2, for example, Jung et al. [16] air-dried poplar samples overnight.

Table 1. Various extraction techniques use on lignocellulosic biomass prior to time-of-flight secondary ion mass spectrometry analysis.

Solvent(s)	Extraction method
Acetone	Soxhlet extract with acetone-water (9:1, v:v) overnight or for 48 h [13, 17].
Dichloromethane	Soxhlet extracted with dichloromethane overnight [16].
Ethanol, acetone, and water	Dehydration in a series of ethanol-water (20, 40, 60, 80, 100% v/v) for 10 min each, 1:1 acetone-ethanol solution, and pure acetone [34].
Ethanol, toluene, and water	Soxhlet extract with 1.0 L absolute ethanol and 427 mL toluene for 4 h followed by ethanol for 4 h or longer [12].
	95% ethanol for 4–5 h, ethanol-toluene (2:1 or 7:3) for 6–8 h, and boiling water for 3 h [10, 12].

Table 2. Four drying technique and procedural details used by Tokareva et al. [29].

Drying technique	Details
Air drying	Ambient temperature for 3 days
Critical point drying	CO_2 transition fluid
Freeze drying	20 h
Nitrogen flow drying	Room temperature

Lignocellulosic Secondary Ion Peaks

Various studies were conducted to determine the key ion peaks characterizing lignocellulosic components and develop a ToF-SIMS library for biomass. In 2003, Fardim and Durán proposed a list of tentative peak assignments for the ToF-SIMS-positive secondary ions from unbeaten and beaten pulp derived from *Eucalyptus grandis* wood chips [32]. Those peak assignments represented cellulose (*m/z* 127 and 145), xylan (*m/z* 115 and 133), and lignin (*m/z* 137, 151, 167, and 181) [32]. The processes for deriving the representative peaks for lignin, cellulose, and hemicellulose from isolated lignocellulosic components are addressed below.

Lignin

Fardim and Durán [32] tentatively proposed that the secondary ions representing lignin ToF-SIMS peaks of *m/z* 137, 151, 167, and 181 were $C_8H_9O_2^+$, $C_8H_7O_3^+$, $C_9H_{11}O_3^+$, and $C_9H_9O_4^+$, respectively. To verify these peaks, it was necessary to first analyze isolated lignin samples and then the lignin in the biomass. Also, the sources of the biomass lignin were varied as softwoods predominately have guaiacyl (G) lignin, whereas hardwoods are primarily composed of guaiacyl (G) and syringyl (S) lignin, and grasses contain all three types – *p*-hydroxyphenyl (H), guaiacyl (G), and syringyl (S) lignin. The structures of the three monolignol

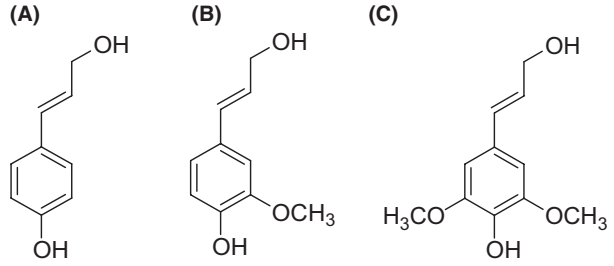

Figure 4. Three monolignol: (A) *p*-coumaryl alcohol, (B) coniferyl alcohol, and (C) sinapyl alcohol.

that H, G, and S lignin are derived from are illustrated in Figure 4.

Various studies were conducted on milled wood lignin (MWL) [14, 20], Klason lignin [35], and lignin model dimers [11]. The analysis of pine and spruce MWL revealed lignin characteristic peaks in the spectra at *m/z* 137 and 151, which correlates with G lignin [14, 35]. The peak at *m/z* 137 does represent $C_8H_9O_2^+$ as Fardim and Durán tentatively assigned [14, 32]; however, based on the spectra of pine MW led Saito et al. [14] to conclude that *m/z* 151 actually was two unresolved peaks, $C_8H_7O_3^+$ and $C_9H_{11}O_2^+$. The two peaks were able to be resolved when they analyzed unlabeled coniferyl alcohol [14]. All of the ToF-SIMS G lignin ions were confirmed by using deuterium-labeled synthetic lignin, DHP [14]. The chemical structure for the G lignin ions can be found in Table 3.

Using lignin model dimer compounds, it was determined that the interunit linkages of 8-O-4', 8-1', 8-8', and 8-5' contributed to the formation of G lignin fragmentation ions (*m/z* 137 and 151) and that those peaks can originate from the phenolic end group or the ether-linked phenolic unit of a lignin polymer with a 8-O-4' linkage, as illustrated in Scheme 1 [11].

Beech MWL also revealed G lignin ion peaks in addition to characteristic peaks of S lignin at *m/z* 167

Table 3. Mass-to-charge ratio, chemical formula, and chemical structure of lignin fragmentation ions in biomass for time-of-flight secondary ion mass spectrometry analysis [20].

Mass-to-charge ratio (*m/z*)	Chemical formula	Chemical structure	Characterization
107	$C_7H_7O^+$	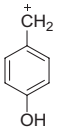	H lignin
121	$C_7H_5O_2^+$, $C_8H_9O^+$	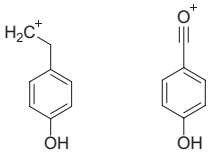	H lignin
137	$C_8H_9O_2^+$	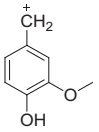	G lignin
151	$C_8H_7O_3^+$, $C_9H_{11}O_2^+$	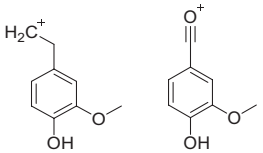	G lignin
167	$C_9H_{11}O_3^+$	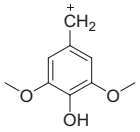	S lignin
181	$C_9H_9O_4^+$, $C_{10}H_{13}O_3^+$	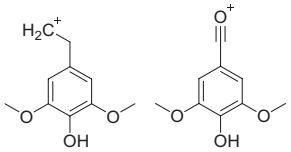	S lignin

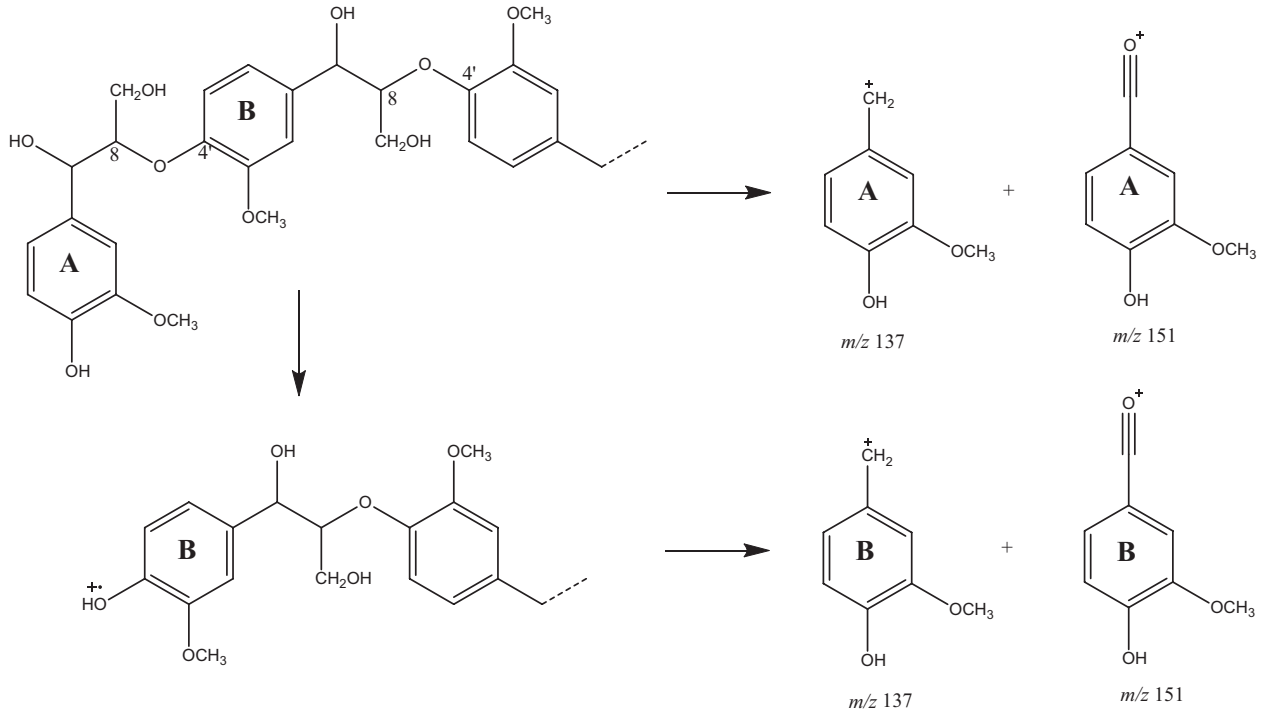

Scheme 1. A postulated fragmentation pathway to the formation of G lignin ions at *m/z* 137 and 151 originating from the phenolic end group (A) or the ether-linked phenolic unit (B) with a 8-O-4′ linkage [11].

and 181 (Fig. 5). The former peak represents $C_9H_{11}O_3^+$ while the latter peak was also an unresolved double peak characterizing $C_9H_9O_4^+$ and $C_{10}H_{13}O_3^+$ (Table 3) [14].

Time-of-flight secondary ion mass spectrometry analysis of two lignin dimeric compounds composed of a G unit and H unit, 1-(4-hydroxyphenyl)-1-hydroxy-2-(2-methoxyphenoxy)-ethane and 1-(4-hydroxyphenyl)-1-ethoxy-2-(2-methoxyphenoxy)-ethane, resulted in distinct peaks at *m/z* 107 and 121 [35]. Another ToF-SIMS study, the spectrum of wheat straw Klason lignin revealed peaks representing H, G, and S lignin, and where the ion counts for the H lignin peaks (*m/z* 107 and 121) were more intense than that of G and S lignin [35]. It was determined through high mass resolution that the H lignin ion peak (*m/z* 121) could be resolved into two peaks, $C_7H_5O_2^+$ and $C_8H_9O^+$, (Table 3) [20]. Spectra of both aspen Klason lignin and a hardwood aspen section interestingly revealed the H lignin peak at *m/z* 121, but not *m/z* 107 [35].

Lignin ion peaks in the ToF-SIMS spectra for wood are less intense compared to the synthesized lignin, and most likely caused by the cell wall matrix [20]. This matrix contains both covalent and noncovalent cross-linkages

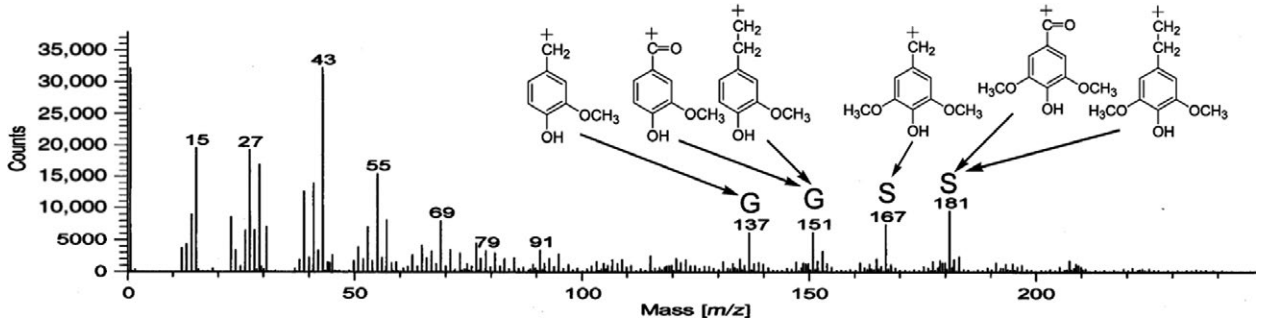

Figure 5. Time-of-flight secondary ion mass spectrometry spectra of beech MWL. Reprinted (adapted) with permission from Saito et al. [14]. Copyright (2005) American Chemical Society.

Table 4. Lignin and polysaccharide peak list [13, 22].

Lignin		Polysaccharide	
Mass	Exact mass	Mass	Exact mass
51	51.021	44[1]	44.023[1]
63	63.022	47	47.013
65	65.038	59[1]	59.015[1]
67	67.056	60[1]	60.021[1]
77	77.037	61	61.030
79	79.056	71	71.014
91	91.051	81	81.036
93	93.073	83[1]	83.013[1]
95[1]	95.092[1]	85[1]	85.034[1]
105	105.071	87[1]	87.051[1]
107	107.044	97	97.032
115	115.045	99	99.049
121	121.065	101[1]	101.029[1]
128	128.051	109	109.033
137	137.063	113	113.026
151	151.049	127	127.041
152	152.050	145	145.061
153	153.049		
165	165.059		
167	167		
181	181		
189	189.059		

[1]Protein fragment interference.

between lignin and cellulose and hemicellulose [20]. Goacher et al. studied red pine and developed a more comprehensive list for lignin (Table 4) other than the six characteristic peaks that represent H, G, and H lignin ion [13, 22]. Polydimethyl siloxane (PDMS) contamination interference resulted in a few of the peaks at *m/z* 15, 45, 73, 131, and 147 to be removed from the original list due to potential peak overlap [22]. Two peaks, *m/z* 19 and 31, were also removed from the original list due to dependence on the sample moisture content [22]. If the biomass sample was previously treated with proteins, like cellulase and laccase, there will also be protein interference with some lignocellulosic peaks; these peaks are noted by an asterisk in Table 4 and should not be included in the analysis under these or similar conditions [22]. The normalized ion intensities of the lignin ion

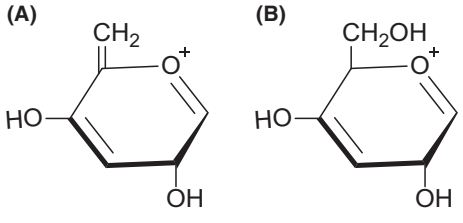

Figure 6. The chemical structures for cellulose ions (A) *m/z* 127 and (B) *m/z* 145 [44].

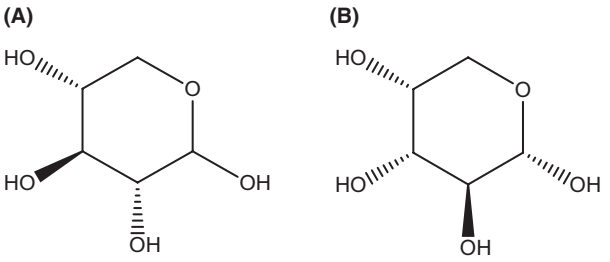

Figure 7. The chemical structures (A) D(+)-xylose and (B) D(−)-arabinose.

peaks in Table 4 can be used to calculate the lignin peak fraction (Eq. 1), lignin modification metric (Eq. 2), or the polysaccharide peak fraction (Eq. 3), where L and PS are the sums of lignin and polysaccharide peaks, respectively, in Table 4. The lignin modification metric (Eq. 2) helps determine the relative amount of lignin benzene rings that lose methoxy groups that are present in G and S lignin units; the G and S in equation 2 represent G lignin and S lignin peaks in Table 3, whereas Ar represents the sum aromatic peaks of *m/z* 77 and 91 [21, 22].

$$\text{Lignin peak fraction} = \frac{L}{L+PS}, \tag{1}$$

$$\text{Lignin modification metric} = \frac{G+S}{\text{Ar}}, \tag{2}$$

$$\text{Polysaccharide peak fraction} = \frac{PS}{PS+L}. \tag{3}$$

The use of this comprehensive list (Table 4) is typically not used for ToF-SIMS images because it would result in an overwhelming number of selected ion images that would be difficult to sum up for PS and L images. For ToF-SIMS lignin ion images, the major contributing ions for H, G, and S lignin (Table 3) are used.

Cellulose and hemicellulose

The ToF-SIMS peaks characterizing cellulose can be located in the spectra at *m/z* 127 and 145, which represents ($C_6H_7O_3^+$) and ($C_6H_9O_4^+$), respectively [13]. While there is one report that indicates other hexose compounds, like mannose and galactose, contribute to the assigned cellulose peaks, these two peaks are accepted as representative peaks of cellulose [13, 35]. Figure 6 illustrates the chemical structure of the cellulose-related ions at *m/z* 127 and 145.

Tokareva et al. [35] analyzed D(+)-xylose and D(−)-arabinose (Fig. 7) and determined that peaks at *m/z* 115 ($C_5H_7O_3^+$) and 133 ($C_5H_9O_4^+$) originate from these isolated compounds. With the use of PCA modeling (example seen in Fig. 8), Goacher et al. [13] determined that lignin contributed to *m/z* 115 and neither that peak or *m/z* 133

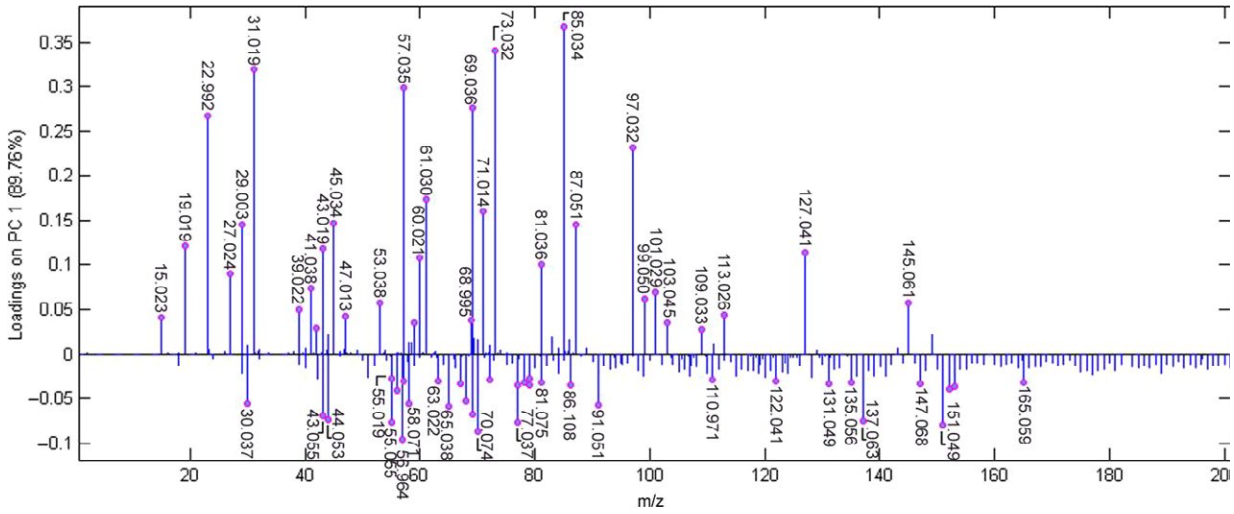

Figure 8. PC1 loading for the PCA model representing ToF-SIMS spectra of extracted red pine, holocellulose, and cellulose fractions. Reprinted (adapted) with permission from Goacher et al. [13]. Copyright (2011) American Chemical Society.

distinguished holocellulose from α-cellulose or a pine wood. This means that while these two peaks could be characteristic peaks for hemicellulose in isolated xylose, they cannot be used to represent carbohydrates when analyzing pine wood [13]. While this study occurred only with softwood pine sample, it is not recommended to use *m/z* 115 and 133 to represent hemicellulose in any biomass.

As mentioned above, while Goacher et al. [13] developed a comprehensive ToF-SIMS peak list for lignin characteristic peaks, they also verified a list for polysaccharide characteristic peaks (Table 4) through PCA modeling. This list can be used to calculate the polysaccharide or the lignin peak fraction (Eqs. 1 and 3). The original polysaccharide peak list, like the lignin list, had a few peaks removed due to PDMS contamination or their dependence on moisture content; similarly, specific peaks (denoted by an asterisk in Table 4) should not be used after enzymatic activity on the biomass because of protein interference with these polysaccharide ToF-SIMS peaks [13, 22].

Extractives and pectins

While biomass needs to be extracted to obtain accurate lignin and polysaccharide peaks intensities, there have been some studies conducted on identifying some of the fragmentation peaks for extractives. As mentioned in the biomass sample preparation section on removing the extractives, 18 extractives with proposed peak assignments over *m/z* 200 and a list of peaks under *m/z* 200 that "distinguished unextracted from extracted lignocelluloses samples" were determined by Fardim and Durán and Goacher et al. [12, 32]. Imai et al. [36] was able to identify a high-intensity ion peak at *m/z* 285 in Sugi heartwood tissue that corresponds to the diterpene phenol ferruginol. As extractives overlap the lignin content peaks, this incorrect increase in lignin intensity would result in a decrease in the polysaccharide peak fraction (Eq. 3) for unextracted biomass [12]. Also, extractives can contribute to the aromatic peak intensity (Ar, *m/z* 77 and 91), resulting in a decrease in the biomass' lignin modification metric (Eq. 2) [12].

Pectins are also naturally occurring heteropolysaccharides in native wood found in the primary cell walls, secondary cell walls, and the middle lamella [35, 37]. Tokareva et al. [35] studied pectin by analyzing trigalacturonic acid, polygalacturonic acid, and methyl-esterified pectin. The distinct peak associated with all polymeric pectin models was *m/z* 155, whereas *m/z* 111 correlates with methyl-esterified pectin [35]. Metal ions were also used as markers to label anionic groups, like the carbonyl groups found in some pectins [38]. Metal labeling, using metal ion markers, observed in ToF-SIMS images was most effective

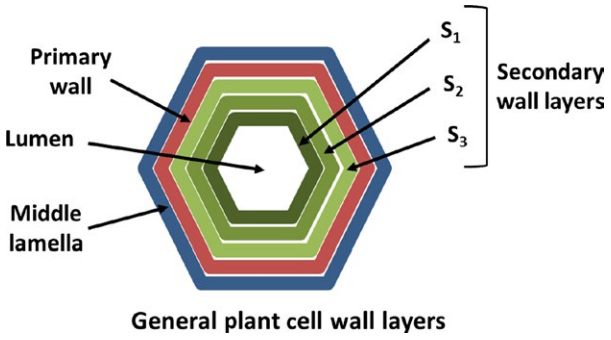

Figure 9. General locations of the plant cell walls layers: middle lamella, primary cell wall, secondary cell walls, and the lumen.

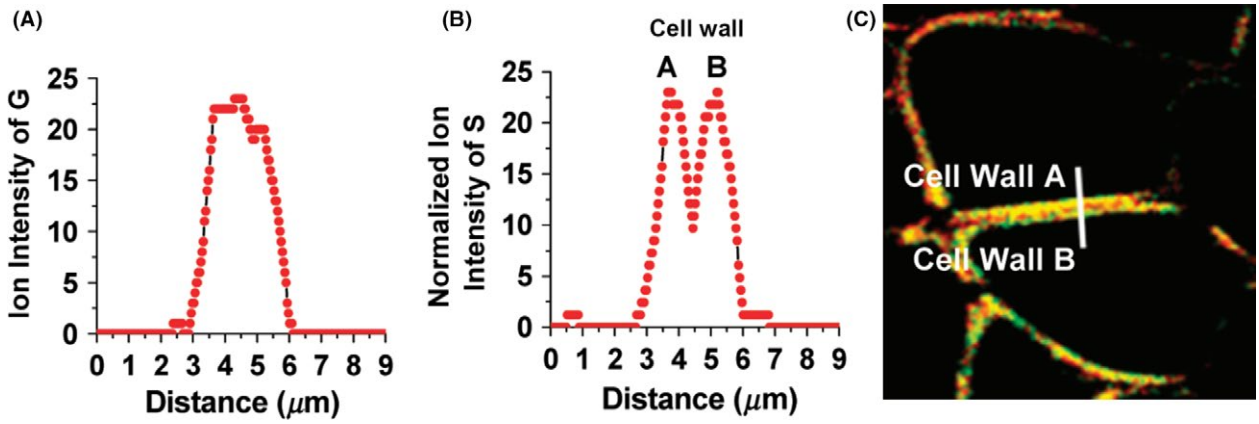

Figure 10. Line intensity profiles for (A) G lignin ions and (B) S lignin ions across (C) the fiber cell wall from A to B. Reprinted (adapted) with permission from Zhou et al. [25]. Copyright (2011) American Chemical Society.

using Sr^{2+} ions, but that Cu^{2+} ion also identified itself as a useful marker [38].

Origination of Components in the Cell Wall

Spatial mapping is extremely useful in identifying the location lignocellulosic fragmentation ions originate from within the cell wall (Fig. 9). The cell wall thickness was automatically estimate by Gerber et al. [30], although the combination of computational modeling and ToF-SIMS analysis to develop an "artificially created cell wall mask." The average cell wall thickness of a 5-year-old field-grown poplar transversal section via ToF-SIMS analysis was 7.6 ± 0.4 μm [30]. This average includes the fiber cell walls of the thicker late wood, thus resulting in a slightly higher value than the 5.4 μm average found in literature [30]. This technique can further be used to differentiate cell wall thickness between wild-type and genetically modified biomass.

Typical locations for high-intensity lignin ions are in the secondary cell wall and the cell corners regions [24]. More specifically, Zhou et al. [25] used ToF-SIMS line intensity profiles (Fig. 10) to illustrate the predominant locations of G lignin and S lignin in the cell walls, which are the middle lamella and the secondary cell walls, respectively. In relation to specific cells, it was determined that poplar vessel cell walls have more G lignin than fiber cell walls [25]. A lower S/G lignin ratio is the result of higher G lignin in the vessel cells [25]. Vessel cells closer to fiber cells have a S/G ratio of 0.7 compared to the 0.5 of those further from the fiber cells; the fiber cell walls have a 1.1 S/G ratio [25]. These ratio values were interestingly comparable to the S/G ratio for maple, where the vessel walls were approximately 0.6 and maple fiber walls ranged from 0.8 to 1.2 [39]. A different poplar study reported S/G ratio values for the vessel and fiber cells also to be 0.7 and 1.1, respectively [40]. These values are lower than the lowest natural variant poplar S/G ratio of ~1.2 by pyrolysis molecular beam mass spectrometry [41]. S/G ratio for different types of poplars determined by thioacidolysis was also significantly higher than those S/G ratios by the ToF-SIMS above;[42] this difference is most likely a result of the heterogeneous nature of the biomass and the difference in chemistry content on the sample's surface compared to the bulk material. Studying the surface of biomass is important as the amount of cellulose and lignin on the surface may differ from that detected by bulk chemical analysis. This is especially true for biological treatment of biomass, as enzymes and microorganisms typically bind to the surface of biomass.

Most mature woody biomass has heartwood, transition zone, and sapwood, where the dark-colored heartwood is found in the inner core and the pale sapwood is in the outer zone near the bark [28]. The paler transition zone is where extractives accumulate, living cells die, and sapwood becomes heartwood [28]. A study of these three different areas in Hinoki cypress (*Chamaecyparis obtusa*) revealed that the formation of extractives during the sapwood to heartwood transition occurred within the ray parenchyma cells [28]. The ToF-SIMS was used to track the relative intensity of elements Na, Mg, Al, K, and Ca from heartwood to sapwood [28]. Saito et al. [28] showed that heartwood had a higher concentration of K and relatively lower concentrations of Na, Mg, Al, and Ca compared to the sapwood with a "drastic increase or decrease" of Na, Al, and Ca distribution in the transition zone.

As mentioned above in the section on extractives and pectins, Tokareva et al. [38] used metal ion

Table 5. List of softwoods, hardwoods, and grasses analyzed by the time-of-flight secondary ion mass spectrometry.

Softwoods	Hardwoods	Grasses
Pine [13, 17, 23]	Poplar [16, 24, 25, 30]	Rice straw [21]
Spruce [12, 22, 29, 33–35]	Birch [17]	Reed [18]
Cedar [19]	Aspen [12, 22, 34, 35]	*Arabidopsis* [10]
Fir [23]		
Cypress [28]		
Beech MWL [20]		

markers to determine the location of anionic groups within the biomass; these anionic groups can provide insight into the location of pectins and xylan. Sr^{2+}-labeled anionic groups were detected in the ray cells and pit membranes of spruce using ToF-SIMS images [38]. ToF-SIMS images further suggested that more methyl-esterified pectin can be found in the ray cells than the pit membrane regions [38]. Analysis with Sr^{2+} labeling revealed that pectins remain in the ray cells and pit membranes of spruce even after delignification [38]. In general, pectin can be found in ray cells, primary cell walls, cell corners, and near the pits of biomass [38]. ToF-SIMS images of the ferruginol fragment peak at *m/z* 285 revealed that it is distributed relatively evenly throughout the inside and along the walls of the axial and ray parenchyma cells in addition to the tracheid cell walls [36].

Chemical, Biological, and Genetic Modification in Biomass

Biomass modification can occur through chemical pretreatments, microbial treatments, and genetic modifications. A list of softwoods, hardwoods, and grasses analyzed by ToF-SIMS can be seen in Table 5.

Chemical pretreatment

Oftentimes, chemical pretreatments are needed to reduce the natural recalcitrance of the biomass in order to facilitate subsequent enzymatic deconstruction. Pretreatments tend to solubilize lignin and/or hemicellulose, but different methods could alter the properties of lignin and negatively impact the glucan digestibility [43]. The changes to the physical cell walls also can occur during pretreatments and research showed that increasing the sample surface area is more important than lignin removal when striving for higher sugar yields after enzymatic hydrolysis [6]. The biomass chemistry and/or cell walls morphology alterations depending on the chemical treatments; analysis of the surface chemistry provides insight into the efficiency of the pretreatment and the impact it has on the cell walls by detecting the changes to the cell wall chemistry. ToF-SIMS can also reveal lignin migration from one area of the cell wall to another and through an increase in cellulose ions on the surface it can indicate if the pretreatment improved the accessibility of cellulose. The different chemical pretreatments and conditions for biomass that have been subsequently analyzed by the ToF-SIMS are listed in Table 6.

Generally, mild thermochemical alkali pretreatment improves enzymatic digestibility through the solubilization of lignin and hemicellulose [21]. A study analyzed the impact of washing with water or HCl of rice straw after an alkaline pretreatment (Table 6) [21]. It was determined that lignin was removed through the alkali pretreatment process, but was redeposited onto the surface due to the acid wash; this can be seen in the increase of approximately 9.7% in acid-washed lignin peak fraction (Eq. 1) compared to water-washed sample [21]. The ToF-SIMS analysis was useful for providing insight into the changes occurring on the surface of the sample that is not always clear from the bulk compositional analysis.

Table 6. Chemical pretreatments and conditions of biomass, where the biomass samples are later analyzed by the time-of-flight secondary ion mass spectrometry.

Pretreatment	Conditions	Author
Alkaline	NaOH (1.5 g/g sample) in pressure tube at 121°C for 1 h	Karuna et al. [21]
	NaOH (0.2 g/g substrate), liquor/solid (w/w) 10:1, 60°C for 2 h	Mou et al. [18]
Alkaline peroxide	NaOH (0.2 g/g substrate) and H_2O_2 (0.25 g/g substrate), liquor/solid (w/w) 10:1, dark place at room temperature for 24 h	Mou et al. [18]
Dilute Acid (DAP) Severe DAP	1 vol% H_2SO_4 in batch reactor at 160°C for 10 min	Jung et al. [16]
	2 vol% H_2SO_4 in batch reactor at 175°C for 10 min	
Holocellulose Severe Holocellulose	$NaClO_2$ (1.30 g/g sample) in 0.14 M CH_3OOH at 70°C for 1 h (x3)	Jung et al. [16]
	$NaClO_2$ (1.30 g/g sample) in 0.14 M CH_3OOH at 70°C for 1 h (x6)	
Hydrotropic[1]	30% (w/v) SXS at 150°C for 30 min or 2 h	Mou et al. [17]
	30% (w/v) SXS and 0.17% (w/v) formic acid, liquor solid (w/w) 10:1) at 160°C 60 min, pH = 3.5 ± 0.05	Mou et al. [18]

[1]Sodium xylene sulfonate (SXS).

A comparison study among alkaline, alkaline peroxide, and hydrotropic pretreated common reed samples revealed that hydrotropic pretreatment was more efficient at removing hemicelluloses and increasing the glucan percentage through bulk compositional analysis [18]. ToF-SIMS analysis revealed that the most efficient enzymatic hydrolysis occurred with the hydrotropic pretreated sample; the enzymatically hydrolyzed hydrotropic sample was lower 58.1% and 64.3% for the carbohydrates/lignin ratio and the guaiacyl/total lignin ratio, respectively, compared to the pretreated sample [18]. Through ToF-SIMS images, it was determined that residual lignin location on the surface fiber changed after the pretreatments and that decrease in lignin allowed for more carbohydrates to be exposed [18]. Now, the carbohydrate ToF-SIMS data should be used carefully as the authors used *m/z* 115 and 133 peaks in addition to *m/z* 127 and 145 [18], and Goacher et al. [13] determined that *m/z* 115 and 133 do not uniquely identify hemicelluloses in wood. Overall, it was shown through bulk analysis, ToF-SIMS ion intensity ratios, and ToF-SIMS images that hydrotropic pretreatment reduced and even relocalized lignin in the fiber cells of reed [18]. Also, ToF-SIMS analysis was instrumental in determining which pretreatment would be best for enzymatic hydrolysis [18].

Another pretreatment comparison study determined that hydrotropic pretreatment was better at removing lignin and increasing enzyme accessibility than hydrothermal and ionic liquid pretreatments; therefore, birch and pine samples that underwent hydrotropic pretreatment with sodium xylene sulfonate (SXS) for 30 min and 2 h followed by enzymatic hydrolysis were analyzed via ToF-SIMS to determine the changes in surface chemical compositions [17]. The ToF-SIMS analysis of hydrotropic pretreated birch revealed that both lignin and some polysaccharides, most likely low mass hemicelluloses, were being removed from the surface; the loss of polysaccharides mostly occurred in the first 30 min [17]. Comparison between the enzymatically pretreated birch samples and the pretreated birch samples showed that the enzyme treatment possesses the capability of breaking bonds between polysaccharides and lignin as seen in the decrease in lignin ratio (lignin/total ions) [17]. A similar comparison between pretreated and enzymatically pretreated pine lead Mou et al. [17] to believe that lignin–carbohydrate complexes could be influencing the lignocellulosic component fragmentation by the ToF-SIMS. The polysaccharide peak fraction (Eq. 3) did not change after enzymatic hydrolysis for the birch samples, the pine samples did see a 5.0% decrease after enzymatic hydrolysis [17]. There was a 56.1% decrease in lignin/total and a decrease of 18.4% in cellulose/total on the surface after enzymatic hydrolysis of the 2 h hydrotropic pretreated pine sample [17]. For both the birch and the pine, longer pretreatment times reduce the S/G lignin ratio on the surface [17].

Dilute acid pretreatment (DAP) changes the chemistry and cell wall structure of biomass which improves the enzyme accessibility [16]. The conditions for the DAP and severe DAP are in Table 6. Severe DAP sample showed that a significant decrease is S lignin normalized ion counts when compared to the DAP sample; this indicates that S lignin units are easier to breakdown than G lignin units during pretreatment [16]. Cellulose normalized ion counts stayed relatively the same when comparing DAP and severe DAP [16]. Jung et al. [16] did report a 30% increase in xylan on the surface of the sample after DAP, while compositional analysis indicates there is actually a significant decrease in xylose; ToF-SIMS images also revealed what appeared to be xylan migration from the cell wall to middle lamella and the lumen. The lignin contribution to *m/z* 115 might explain the supposed xylan migration to the middle lamella, a typical lignin concentrated region.

Jung et al. [16] also determined there was not a significant differences between holocellulose and severe holocellulose pulping treatment on poplar with regards to the major lignocellulosic compounds via the ToF-SIMS. When compared to the extractive-free poplar sample, the holocellulose and severe holocellulose S lignin relative intensity dropped significantly, whereas the relative G lignin intensity decreased only slightly [16].

Biological treatment with microorganisms

A few studies addressed in the previous section looked at the efficiencies of various pretreatments and pretreatments followed by enzymatic hydrolysis [17, 18, 21]. Enzyme activity will result in modification or degradation of biomass and the ToF-SIMS is a useful tool to monitor the changes that occur [33]. The adjustments to the lignocellulosic library (Table 4) that would account for protein interference in the ToF-SIMS spectra as a result of enzyme activity was determined by studying the impact both laccase and cellulase had on white spruce and trembling aspen [22]. Cellulase treatment increased lignin and decreased polysaccharides on the surface, as seen by the 19% and 34% drop in polysaccharide peak fraction (Eq. 3) for aspen and spruce, respectively [22]. Laccase activity, with a mediator, cleaved the "hydroxyl and methoxy groups from lignin benzoid units" and resulted in a reduction in both G and S lignin peak intensity [22]. Another study reported that high laccase dosage allows the protein to penetrate the biomass and reduce the polysaccharide content [26].

While biomass extractives will alter the analysis of surface lignocellulose peaks by overlapping with lignin peaks, a cellulase enzyme treatment can still be detected on unextracted wood [12]. The cellulase enzyme activity was detected using PCA modeling of the ToF-SIMS ions from

Celluclast-treated unextracted and extracted red spruce [12].

A way to significantly minimize or even eliminate contamination during processing is to conduct the fiber-based enzyme assays in a 96-well filter plate [12]. Another potential issue with enzymatic activity on biomass is through buffer interference, which was addressed by rinsing in the section on sample preparation [33].

Principal component analysis modeling of ToF-SIMS spectra and images from white rot fungus (*Phanerochaete carnosa*) treated balsam fir and lodgepole pine wood detected prominent polysaccharide peaks, while lignin peaks strongly characterized the control samples; this indicates lignin degradation on the surface of the treated sample [23]. The decrease in lignin simultaneously results in an increase in polysaccharide ions on the wood surface [23]. The ToF-SIMS images indicate that lignin removal does not occur predominately in the middle lamella and cell corners, but across the cell walls [23]. Interestingly, Mahajan et al. [23] were able to determine that the fungal decay of pine occurred "more rapidly" than with fir. As softwood lignin is predominantly composed of G lignin and the study showed *P. carnosa*'s ability at targeting and modifying the G lignin, this fungus is a prime candidate at minimizing softwood species' natural recalcitrance [23].

Physical and genetic modification

Stress-induced tension and opposite wood on poplar were studied to determine the chemical differences when compared to normal poplar wood [24]. As expected, there is a relatively low lignin intensity in the gelatinous layer (G-layer) of the tension wood, which is predominately composed of crystalline cellulose; high concentration of lignin was found in the secondary cell wall and the cell corner regions [24]. Other than the increased intensity of cellulose ions in the G-layer, cellulose is rather evenly distributed over the tension wood surface [24]. Jung et al. conducted 3D analysis from 30 sputtering cycles with O_2^+ on the tension wood and a line scan across a region of interest. The line scan bisects a G-layer, secondary cell wall, and a cell corner, and confirms that cellulose is observed in the G-layer and lignin signal is relatively high in the other two areas [24].

Genetically modified biomass will typically have anatomical changes, which will usually impact the chemistry of the biomass [30]. PCA modeling of the ToF-SIMS spectra data was able to determine that wild-type *Arabidoposis* (*A. thaliana* Col-0) was enriched in S lignin, while the *Arabidopsis fah1* mutant had a significant amount of G lignin; these data are consistent with our understanding that the *fah1* lines halt the production of S lignin and its incorporation into the cell wall [10]. The high S lignin content found in the fiber cells of the wild type contributes to the higher S/G lignin ratio compared to the *fah1* mutant [10]. The polysaccharide peak fraction (Eq. 3) indicates that the difference between the wild type and the mutant is not associated with carbohydrates [10]. Now, the *Arabidopsis irx3* mutation does result in approximately 20% depletion of cellulose, and the polysaccharide peak fraction ratio similarly reports a decrease of 15% between the wild type and this mutant [10]. This shows that the ToF-SIMS is capable of differentiating genetic mutations of herbaceous plants.

Genetic modifications in poplar by downregulating the *PdKOR2* gene resulted in a S/G ratio decrease of approximately 50% on the fiber cell walls and less than 10% S/G ratio increase on the vessel cell walls. The ToF-SIMS analysis of the overall S/G ratio for the transgenic sample compared to the control was lower. It was shown that while the bulk chemical analysis can provide insight into the changes to a plant due to genetic modifications, surface characterization can reveal alterations occurring to specific types of plant cells and cell wall layers [40].

Summary and Future Applications

While the ToF-SIMS does not provide quantitative data, it is a useful instrument capable of detecting and mapping lignocellulosic ions on the surface of various biomasses. It is a valuable analytical technique to incorporate into pretreatment, microbial/enzymatic treatment, and genetic modification studies in order to understand the chemical changes occurring to the surface of the biomass. In the future, ToF-SIMS analysis can be utilized in microbial and enzymatic treatment studies by determining the change in surface chemistry over time; three-dimensional imaging can also assist in discerning the depth microorganisms and enzymes penetrate the sample and impact the chemistry of the biomass. ToF-SIMS analysis also has potential to be used in pretreatment enzymatic hydrolysis studies to assist in optimizing the chemical pretreatment process in order to produce the most effective hydrolysis yields. Using the ToF-SIMS in preliminary studies to narrow a large sample set could potentially save time, chemicals, and samples. While the ToF-SIMS is an extremely useful tool for surface analysis, additional studies are needed to compare it with other techniques, including fluorescence imaging, Ramen spectroscopy, and infrared spectroscopy. A few studies have incorporated additional surface analysis techniques, like scanning electron microscopy, in conjunction with the ToF-SIMS; a few studies incorporated multiple analysis methods that detect physical and chemical changes to a sample could provide valuable insight into ways to efficiently utilize lignocellulosic biomass [16, 19, 24]. Kuroda et al. [19] specifically

analyzed the distribution of chemicals on frozen hydrated using a cryo-ToF-SIMS/SEM system, a similar system could be developed to analyze the physical and chemical surface at the same location of the biomass in an enzymatic or microbial study. Nevertheless, as research continues into the use of lignocellulosic chemical components, specifically lignin, for biomaterials and biofuels, the ToF-SIMS will be a vital asset in detecting chemical changes on the material surface along with spatial mapping.

Acknowledgments

This manuscript has been authored by UT-Battelle, LLC, under contract no. DE-AC05-00OR22725 with the U.S. Department of Energy. The BioEnergy Science Center is supported by the Office of Biological and Environmental Research in the U.S. Department of Energy. Mass spectrometry analysis was carried out by the U.S. Department of Energy Office of Biological and Environmental Research supported Bioenergy Research Center proteomics pipeline. The publisher, by accepting the article for publication, acknowledges that the United States Government retains a nonexclusive, paid-up, irrevocable, world-wide license to publish or reproduce the published form of this manuscript, or allow others to do so, for United States Government purposes. The Department of Energy will provide public access to these results of federally sponsored research in accordance with the DOE Public Access Plan (http://energy.gov/downloads/doe-public-access-plan). A.K.T. is grateful for the financial support from the Paper Science & Engineering (PSE) fellowship program at the Renewable Bioproducts Institute at Georgia Institute of Technology.

Conflict of Interest

None declared.

References

1. Sun, Q., M. Foston, X. Meng, D. Sawada, S. V. Pingali, H. M. O'Neill et al. 2014. Effect of lignin content on changes occurring in poplar cellulose ultrastructure during dilute acid pretreatment. Biotechnol. Biofuels 7:1.
2. Yáñez-S, M., B. Matsuhiro, C. Nunez, S. Pan, C. A. Hubbell, P. Sannigrahi et al. 2014. Physicochemical characterization of ethanol organosolv lignin (EOL) from Eucalyptus globulus: Effect of extraction conditions on the molecular structure. Polym. Degrad. Stab. 110:184–194.
3. Zhang, W., Z. Yi, J. Huang, F. Li, B. Hao, M. Li et al. 2013. Three lignocellulose features that distinctively affect biomass enzymatic digestibility under NaOH and H2SO4 pretreatments in Miscanthus. Bioresour. Technol. 130:30–37.
4. Hong, J., X. Ye, and Y. H. P. Zhang. 2007. Quantitative determination of cellulose accessibility to cellulase based on adsorption of a nonhydrolytic fusion protein containing CBM and GFP with its applications. Langmuir 23:12535–12540.
5. Wang, Q. Q., Z. He, Z. Zhu, Y. H. P. Zhang, Y. Ni, X. L. Luo et al. 2012. Evaluations of cellulose accessibilities of lignocelluloses by solute exclusion and protein adsorption techniques. Biotechnol. Bioeng. 109:381–389.
6. Rollin, J. A., Z. Zhu, N. Sathitsuksanoh, and Y. H. P. Zhang. 2011. Increasing cellulose accessibility is more important than removing lignin: A comparison of cellulose solvent based lignocellulose fractionation and soaking in aqueous ammonia. Biotechnol. Bioeng. 108:22–30.
7. Donohoe, B. S., S. R. Decker, M. P. Tucker, M. E. Himmel, and T. B. Vinzant. 2008. Visualizing lignin coalescence and migration through maize cell walls following thermochemical pretreatment. Biotechnol. Bioeng. 101:913–925.
8. Li, C., B. Knierim, C. Manisseri, R. Arora, H. V. Scheller, M. Auer et al. 2010. Comparison of dilute acid and ionic liquid pretreatment of switchgrass: biomass recalcitrance, delignification and enzymatic saccharification. Bioresour. Technol. 101:4900–4906.
9. Zhu, Z., N. Sathitsuksanoh, T. Vinzant, D. J. Schell, J. D. McMillan, and Y. H. P. Zhang. 2009. Comparative study of corn stover pretreated by dilute acid and cellulose solvent-based lignocellulose fractionation: Enzymatic hydrolysis, supramolecular structure, and substrate accessibility. Biotechnol. Bioeng. 103:715–724.
10. Tsai, A. Y. L., R. E. Goacher, and E. R. Master. 2015. Detecting changes in arabidopsis cell wall composition using time-of-flight secondary ion mass spectrometry. Surf. Interface Anal. 47:626–631.
11. Saito, K., T. Kato, H. Takamori, T. Kishimoto, and K. Fukushima. 2005. A new analysis of the depolymerized fragments of lignin polymer using ToF-SIMS. Biomacromolecules 6:2688–2696.
12. Goacher, R. E., A. Y.-L. Tsai, and E. R. Master. 2013. Towards practical time-of-flight secondary ion mass spectrometry lignocellulolytic enzyme assays. Biotechnol. Biofuels 6:1.
13. Goacher, R. E., D. Jeremic, and E. R. Master. 2011. Expanding the library of secondary ions that distinguish lignin and polysaccharides in time-of-flight secondary ion mass spectrometry analysis of wood. Anal. Chem. 83:804–812.
14. Saito, K., T. Kato, Y. Tsuji, and K. Fukushima. 2005. Identifying the characteristic secondary ions of lignin polymer using ToF-SIMS. Biomacromolecules 6:678–683.

15. Belu, A. M., D. J. Graham, and D. G. Castner. 2003. Time-of-flight secondary ion mass spectrometry: techniques and applications for the characterization of biomaterials surface. Biomaterials 24:3635–3653.
16. Jung, S., M. Foston, M. C. Sullards, and A. J. Ragauskas. 2010. Surface characterization of dilute acid pretreated Populus deltoides by ToF-SIMS. Energy Fuels 24:1347–1357.
17. Mou, H.-Y., E. Orblin, K. Kruus, and P. Fardim. 2013. Topochemical pretreatment of wood biomass to enhance enzymatic hydrolysis of polysaccharides to sugars. Bioresour. Technol. 142:540–545.
18. Mou, H. Y., E. Heikkilä, and P. Fardim. 2013. Topochemistry of alkaline, alkaline-peroxide and hydrotropic pretreatments of common reed to enhance enzymatic hydrolysis efficiency. Bioresour. Technol. 150:36–41.
19. Kuroda, K., T. Fujiwara, T. Imai, R. Takama, K. Saito, Y. Matsushita et al. 2013. The cryo-TOF-SIMS/SEM system for the analysis of the chemical distribution in freeze-fixed Cryptomeria japonica wood. Surf. Interface Anal. 45:215–219.
20. Saito, K., T. Kato, H. Takamori, T. Kishimoto, A. Yamamoto, and K. Fukushima. 2006. A new analysis of the depolymerized fragments of lignin polymer in the plant cell walls using ToF-SIMS. Appl. Surf. Sci. 252:6734–6737.
21. Karuna, N., L. Zhang, J. H. Walton, M. Couturier, M. H. Oztop, E. R. Master et al. 2014. The impact of alkali pretreatment and post-pretreatment conditioning on the surface properties of rice straw affecting cellulose accessibility to cellulases. Bioresour. Technol. 167:232–240.
22. Goacher, R. E., E. A. Edwards, A. F. Yakunin, C. A. Mims, and E. R. Master. 2012. Application of Time-of-Flight-Secondary Ion Mass Spectrometry for the detection of enzyme activity on solid wood substrates. Anal. Chem. 84:4443–4451.
23. Mahajan, S., D. Jeremic, R. E. Goacher, and E. R. Master. 2012. Mode of coniferous wood decay by the white rot fungus Phanerochaete carnosa as elucidated by FTIR and ToF-SIMS. Appl. Microbiol. Biotechnol. 94:1303–1311.
24. Jung, S., M. Foston, U. C. Kalluri, G. A. Tuskan, and A. J. Ragauskas. 2012. 3D chemical image using TOF-SIMS revealing the biopolymer component spatial and lateral distributions in biomass. Angew. Chem. Int. Ed. 51:12005–12008.
25. Zhou, C., Q. Li, V. L. Chiang, L. A. Lucia, and D. P. Griffis. 2011. Chemical and spatial differentiation of syringyl and guaiacyl lignins in poplar wood via time-of-flight secondary ion mass spectrometry. Anal. Chem. 83:7020–7026.
26. Jeremic, D., R. E. Goacher, R. Yan, C. Karunakaran, and E. R. Master. 2014. Direct and up-close views of plant cell walls show a leading role for lignin-modifying enzymes on ensuing xylanases. Biotechnol. Biofuels 7:1.
27. Sodhi, R. N. 2004. Time-of-flight secondary ion mass spectrometry (TOF-SIMS):- versatility in chemical and imaging surface analysis. Analyst 129:483–487.
28. Saito, K., T. Mitsutani, T. Imai, Y. Matsushita, A. Yamamoto, and K. Fukushima. 2008. Chemical differences between sapwood and heartwood of Chamaecyparis obtusa detected by ToF-SIMS. Appl. Surf. Sci. 255:1088–1091.
29. Tokareva, E., P. Fardim, A. Pranovich, H.-P. Fagerholm, G. Daniel, and B. Holmbom. 2007. Imaging of wood tissue by ToF-SIMS: Critical evaluation and development of sample preparation techniques. Appl. Surf. Sci. 253:7569–7577.
30. Gerber, L., V. M. Hoang, L. Tran, H. A. T. Kiet, P. Malmberg, J. Hanrieder et al. 2014. Using imaging ToF-SIMS data to determine the cell wall thickness of fibers in wood. Surf. Interface Anal. 46:225–228.
31. Slutier, A., R. Ruiz, C. Scarlata, J. Sluiter, D. Templeton, and D. Crocker. 2005. Determination of extractives in biomass. National Renewable Energy Laboratory, Golden, CO.
32. Fardim, P., and N. Durán. 2003. Modification of fibre surfaces during pulping and refining as analysed by SEM, XPS and ToF-SIMS. Colloids Surf. A 223:263–276.
33. Braham, E. J., and R. E. Goacher. 2015. Identifying and minimizing buffer interferences in ToF-SIMS analyses of lignocellulose. Surf. Interface Anal. 47:120–126.
34. Tokareva, E. N., A. V. Pranovich, P. Fardim, G. Daniel, and B. Holmbom. 2007. Analysis of wood tissues by time-of-flight secondary ion mass spectrometry. Holzforschung 61:647–655.
35. Tokareva, E. N., A. V. Pranovich, and B. R. Holmbom. 2011. Characteristic fragment ions from lignin and polysaccharides in ToF–SIMS. Wood Sci. Technol. 45:767–785.
36. Imai, T., K. Tanabe, T. Kato, and K. Fukushima. 2005. Localization of ferruginol, a diterpene phenol, in Cryptomeria japonica heartwood by time-of-flight secondary ion mass spectrometry. Planta 221:549–556.
37. Müller-Maatsch, J., M. Bencivenni, A. Caligiani, T. Tedeschi, G. Bruggeman, M. Bosch et al. 2016. Pectin content and composition from different food waste streams. Food Chem. 201:37–45.
38. Tokareva, E. N., A. V. Pranovich, P. Ek, and B. Holmbom. 2010. Determination of anionic groups in wood by time-of-flight secondary ion mass spectrometry and laser ablation-inductively coupled plasma-mass spectrometry. Holzforschung 64:35–43.
39. Saito, K., Y. Watanabe, M. Shirakawa, Y. Matsushita, T. Imai, T. Koike et al. 2012. Direct mapping of morphological distribution of syringyl and guaiacyl

lignin in the xylem of maple by time-of-flight secondary ion mass spectrometry. Plant J. 69:542–552.
40. Tolbert, A. K., T. Ma, U. C. Kalluri, and A. J. Ragauskas. 2016. Determining the syringyl/guaiacyl lignin ratio in the vessel and fiber cell walls of transgenic Populus plants. Energy Fuels 30:5716–5720.
41. Dumitrache, A., H. Akinosho, M. Rodriguez, X. Meng, C. G. Yoo, J. Natzke et al. 2016. Consolidated bioprocessing of Populus using Clostridium (Ruminiclostridium) thermocellum: a case study on the impact of lignin composition and structure. Biotechnol. Biofuels 9:1.
42. Sannigrahi, P., A. J. Ragauskas, and G. A. Tuskan. 2010. Poplar as a feedstock for biofuels: a review of compositional characteristics. Biofuels, Bioprod. Biorefin. 4:209–226.
43. Sathitsuksanoh, N., Z. Zhu, and Y.-H. P. Zhang. 2012. Cellulose solvent-based pretreatment for corn stover and avicel: concentrated phosphoric acid versus ionic liquid [BMIM] Cl. Cellulose 19:1161–1172.
44. Berman, E. S. F., K. S. Kulp, M. G. Knize, L. Wu, E. J. Nelson, D. O. Nelson et al. 2006. Distinguishing Monosaccharide Stereo- and Structural Isomers with TOF-SIMS and Multivariate Statistical Analysis. Anal. Chem. 78:6497–6503.